


RESEARCH

Open Access

# Crosstalk between astrocytes and microglia results in increased degradation of $\alpha$ -synuclein and amyloid- $\beta$ aggregates



Jinar Rostami<sup>1</sup>, Tobias Mothes<sup>1</sup>, Mahshad Kolahehdouzan<sup>2</sup>, Olle Eriksson<sup>3</sup>, Mohsen Moslem<sup>4</sup>, Joakim Bergström<sup>1</sup>, Martin Ingelsson<sup>1</sup>, Paul O'Callaghan<sup>3</sup>, Luke M. Healy<sup>2</sup>, Anna Falk<sup>4</sup> and Anna Erlandsson<sup>1\*</sup> 

## Abstract

**Background:** Alzheimer's disease (AD) and Parkinson's disease (PD) are characterized by brain accumulation of aggregated amyloid-beta (A $\beta$ ) and alpha-synuclein ( $\alpha$ SYN), respectively. In order to develop effective therapies, it is crucial to understand how the A $\beta$ / $\alpha$ SYN aggregates can be cleared. Compelling data indicate that neuroinflammatory cells, including astrocytes and microglia, play a central role in the pathogenesis of AD and PD. However, how the interplay between the two cell types affects their clearing capacity and consequently the disease progression remains unclear.

**Methods:** The aim of the present study was to investigate in which way glial crosstalk influences  $\alpha$ SYN and A $\beta$  pathology, focusing on accumulation and degradation. For this purpose, human-induced pluripotent cell (hiPSC)-derived astrocytes and microglia were exposed to sonicated fibrils of  $\alpha$ SYN or A $\beta$  and analyzed over time. The capacity of the two cell types to clear extracellular and intracellular protein aggregates when either cultured separately or in co-culture was studied using immunocytochemistry and ELISA. Moreover, the capacity of cells to interact with and process protein aggregates was tracked using time-lapse microscopy and a customized "close-culture" chamber, in which the apical surfaces of astrocyte and microglia monocultures were separated by a <1 mm space.

**Results:** Our data show that intracellular deposits of  $\alpha$ SYN and A $\beta$  are significantly reduced in co-cultures of astrocytes and microglia, compared to monocultures of either cell type. Analysis of conditioned medium and imaging data from the "close-culture" chamber experiments indicate that astrocytes secrete a high proportion of their internalized protein aggregates, while microglia do not. Moreover, co-cultured astrocytes and microglia are in constant contact with each other via tunneling nanotubes and other membrane structures. Notably, our live cell imaging data demonstrate that microglia, when attached to the cell membrane of an astrocyte, can attract and clear intracellular protein deposits from the astrocyte.

(Continued on next page)

\* Correspondence: [anna.erlandsson@pubcare.uu.se](mailto:anna.erlandsson@pubcare.uu.se)

<sup>1</sup>Molecular Geriatrics, Rudbeck Laboratory, Department of Public Health & Caring Sciences/, Uppsala University, Uppsala, Sweden

Full list of author information is available at the end of the article



© The Author(s). 2021 **Open Access** This article is licensed under a Creative Commons Attribution 4.0 International License, which permits use, sharing, adaptation, distribution and reproduction in any medium or format, as long as you give appropriate credit to the original author(s) and the source, provide a link to the Creative Commons licence, and indicate if changes were made. The images or other third party material in this article are included in the article's Creative Commons licence, unless indicated otherwise in a credit line to the material. If material is not included in the article's Creative Commons licence and your intended use is not permitted by statutory regulation or exceeds the permitted use, you will need to obtain permission directly from the copyright holder. To view a copy of this licence, visit <http://creativecommons.org/licenses/by/4.0/>. The Creative Commons Public Domain Dedication waiver (<http://creativecommons.org/publicdomain/zero/1.0/>) applies to the data made available in this article, unless otherwise stated in a credit line to the data.

(Continued from previous page)

**Conclusions:** Taken together, our data demonstrate the importance of astrocyte and microglia interactions in A $\beta$ / $\alpha$ SYN clearance, highlighting the relevance of glial cellular crosstalk in the progression of AD- and PD-related brain pathology.

**Keywords:** Alzheimer's disease, Parkinson's disease,  $\alpha$ -Synuclein, Crosstalk, Amyloid- $\beta$ , Astrocyte, Microglia, Co-culture, Degradation, Tunneling nanotube

## Background

The impact of glial cells on pathological processes in various neurodegenerative diseases has recently received much attention. Glial crosstalk is crucial for maintaining brain homeostasis and is believed to play a key role in chronic neuroinflammation. The conversation between microglia and astrocytes starts already during early development and remains throughout life [1]. However, exactly in which way the crosstalk between the two cell types affects the progression of neurodegenerative diseases remains unclear.

Alzheimer's disease (AD) and Parkinson's disease (PD) are the two most common neurodegenerative disorders, characterized by cognitive and functional impairments, which develop over many years. The major pathological hallmarks of the diseases are accumulation of toxic protein aggregates. In PD, intracellular inclusions of alpha-synuclein ( $\alpha$ SYN) are found in neurons and glia, while both extracellular and intracellular deposits of amyloid-beta (A $\beta$ ) are present in the AD brain [2, 3]. Other common features of AD and PD are neuronal cell death and chronic neuroinflammation, involving both innate and adaptive immune responses [4].

In the healthy adult brain, astrocytes are rather stationary cells, forming a well-coordinated network in the parenchyma [5]. Microglia, on the other hand, are motile and constantly sensing the environment around them [6, 7]. In the AD and PD brain, both astrocytes and microglia acquire reactive, inflammatory phenotypes and can effectively phagocytose aggregated proteins and cell debris, as well as secrete various cytokines and inflammatory mediators [8–13]. Up until now, most research has focused on the role of each cell type by itself. However, recent data indicate that microglia and astrocytes coordinate their functions in many ways, both in the healthy and diseased brain [14–21].

Chronic glial activation may contribute to AD/PD progression in several ways, including loss of homeostatic function and gain of toxic functions, causing neuronal loss [22]. In addition, reactive glial cells may be responsible for cell-to-cell spreading of the pathology. We have previously reported that cultured astrocytes accumulate

$\alpha$ SYN and A $\beta$  aggregates but not the monomeric form of the proteins [11, 12]. The  $\alpha$ SYN and A $\beta$  accumulation result in severe cellular stress, indicated by lysosomal and mitochondrial deficiencies [11, 12, 23]. Subsequently, stressed astrocytes respond by sending out tunneling nanotubes (TNTs), enabling intercellular transfer of pathogenic protein aggregates, as well as MHCII complexes to nearby cells [11, 24]. The aim of the present study was to investigate how microglia and astrocytes coordinate their responses in regard to  $\alpha$ SYN and A $\beta$  pathology, including accumulation and degradation of protein aggregates, and cell-to-cell contacts.

## Methods

### Production of alpha-synuclein fibrils

Alpha-synuclein preformed fibrils ( $\alpha$ SYN-F) were generated using endotoxin-free monomeric  $\alpha$ SYN (AnaSpec, A5555-1000) as described previously [24]. Shortly, the monomers were dissolved in PBS at a concentration of 5mg/ml and left on a shaker at 1000 rpm for 7d. Thereafter,  $\alpha$ SYN-F were diluted to a working concentration of 2mg/mL in PBS and stored at  $-80^{\circ}\text{C}$  until use. The  $\alpha$ SYN-F were Cy3-labelled using Cy3<sup>AM</sup> antibody labelling kit (GE Healthcare, PA33000) as described previously [24]. Prior to each experiment, the  $\alpha$ SYN-F were diluted 1:2 in PBS and sonicated twice in 20% amplitude, 1s off and 1s on, for 30s using a Sonics Vibra Cell sonicator.

### Production of amyloid-beta fibrils

Amyloid-beta preformed fibrils (A $\beta$ -F) were generated using human Cy3-labelled A $\beta$ -42 monomers (AnaSpec, 60480-01). The A $\beta$  monomers were dissolved in a 10 mM NaOH/PBS solution to a concentration of 2 mg/ml. The A $\beta$  samples were left to aggregate on a shaker at 1500 rpm,  $37^{\circ}\text{C}$  for 4d. Then, the A $\beta$ -F were diluted using peptide PBS to the final concentration of 0.5 mg/ml and sonicated in 20% amplitude, 1s off and 1s on, for 30s using a Sonics Vibra Cell sonicator.

### Culture of human iPSC-derived astrocytes

Human astrocytes were generated from neuroepithelial-like stem (NES) cells, produced from human-induced

pluripotent stem cells (iPSCs, Cntrl9 cell line) [25, 26]. The NES cells were differentiated in Advanced DMEM/F12 (Thermo Fisher 12634-010) supplemented with 1% penicillin–streptomycin (Thermo Fisher 15140-122), 1% B27 supplement (Thermo Fisher, 11530536), 1% non-essential amino acids (Thermo Fisher, 11140050), and 1% L-glutamine (Thermo Fisher 25030-024). The following factors were added fresh to the medium just before use: basic fibroblast growth factor (bFGF) 10 ng/ml (Thermo Fisher, 13256029), heregulin 10 ng/ml (Sigma Aldrich, SRP3055), activin A 10 ng/ml (Peprotech, 120-14E), and insulin-like growth factor 1 (IGF-1) 200 ng/ml (Sigma Aldrich, SRP3069). Additionally, 20 ng/ml ciliary neurotrophic factor (CNTF; Thermo Fisher, PHC7015) was added to the medium the last 2 weeks of differentiation. Cells were seeded for experiment, at a concentration of 5000 cells/cm<sup>2</sup>, directly after the differentiation protocol was completed.

#### Culturing of human iPSC-derived microglia

To enable co-cultures of human iPSC-derived astrocytes and microglia without strain-induced immunological reactions, microglia were generated from the same human iPSC line that was used for deriving the NES cells. Human iPSCs (Cntrl9 cell line) were cultured in mTeSR Plus medium (Stemcell Technologies, 05825) on matrigel (VWR, 356234)-coated 6-well plates and passaged when an 80% cell density was reached. The iPSCs were passaged using ReLeSR (Stemcell Technologies, 05872), according to the manufacturer's instructions. Generation of hematopoietic progenitor cells (HPCs) and further differentiation to microglia were performed according to the previously published protocol [27], with a few modifications. In short, human iPSCs were seeded at a very low density, and the following day, the mTeSR medium was replaced with medium A (STEMdiff Hematopoietic basal medium supplemented with 1:200 supplement A) (Stemcell Technologies, 05310). After 2d, half of the medium was replaced with fresh medium A. On d3, medium A was completely removed, and medium B (STEMdiff Hematopoietic basal medium supplemented with 1:200 supplement B) was added to the wells. Every other day, 1 ml fresh medium B was added to the cells. On d14, hematopoietic progenitor cells (HPCs) were collected and analyzed with flow cytometry (Fortessa) for the following HPC markers: APC anti-human CD43 (BD Biosciences, 343206) and PE anti-human CD41 (Nordic Biosite, 303706). In addition, the HPCs were stained for Zombie Violet viability dye (Nordic Biosite, 423114) for viability check prior to seeding on matrigel-coated plates. Microglia maturation medium consisted of DMEM F12 (Thermo Fisher, 11039021) supplemented with 2X insulin-transferrin-selenite (Thermo Fisher,

41400045), 2X SM1 (Stemcell Technologies, 5711), 0.5X N2 (Thermo Fisher, 17502048), 1X glutamax (Thermo Fisher, 35050061), 1X non-essential amino acids (Thermo Fisher, 11140050), 400 μM monothio glycerol (Sigma Aldrich, M1753), and 5 μg/mL insulin (Sigma Aldrich, I2643). In addition, the following factors were added to the medium just before use: IL34 (Peprotech, 200-34, 100 ng/mL), MCSF (Peprotech, 300-25, 25ng/mL), IDE1 (Peprotech, 1164899, 10μg/ml). On d24 of microglial differentiation, two additional factors, CX3CL1 (Peprotech, 300-31, 100 ng/mL) and CD200 (Bonopus, C311, 100 ng/mL), were included in the microglia maturation medium. Microglia were plated at the same seeding density as astrocytes (5000 cells/cm<sup>2</sup>) and used for experiments within 14d after completed differentiation.

#### Co-culture of human iPSC-derived microglia and astrocytes

Fully differentiated microglia cells were cultured on matrigel-coated 6-well plates (25,000 cells/well) and left there to adapt for 3d before astrocytes (25,000 cells/well) were added to the culture. Microglia maturation medium supplemented with all the factors both cell types require was used for the co-culture system. Three days after seeding of the astrocytes, co-cultures were exposed to the different treatments.

#### Exposure to αSYN-F and Aβ-F

Astrocytes, microglia, and co-cultures were exposed to 0.5 μM αSYN-F or 0.2 μM Aβ-F for 24h, 4d, or 7d. The concentrations were selected based on our previous studies [11, 12, 23, 28, 29]. The lower concentration of Aβ was used since aggregated Aβ is more toxic to astrocytes than aggregated αSYN. Cell culture media samples from all time points were collected and stored at -80 °C. Additional time-points that were included for the two treatments are described below.

#### αSYN-F

Astrocytes, microglia, and co-cultures were studied at 24h+3d and 24h+6d. After 24h of exposure, cells were washed twice with medium and cultured in αSYN-free medium for additional 3d or 6d.

#### Aβ-F

Astrocytes were studied at 4d+3d. Four days after Aβ-F exposure, astrocytes were washed twice with medium and cultured for additional 3d in Aβ-free medium. Co-cultures were studied at 24h+3d, 24h+6d, and 4d+3d following Aβ-F exposure.

### Conditioned media experiments

For conditioned media experiments, the astrocytes and the microglia cells were treated with  $\alpha$ SYN-F or A $\beta$ -F for 24h. Thereafter, the cells were washed and kept in culture for additional 3d (24h+3d). The conditioned medium from the astrocytes was diluted 1:1 in microglia medium before addition to untreated microglia cultures for 24h. Thereafter, the medium was collected, and cells were fixed. Similarly, conditioned medium from the 24h+3d time point microglia cells was collected and diluted 1:1 in astrocyte medium and added to untreated astrocyte cultures for 24h before medium collection and fixation.

### “Close-culture” chamber system

The close-culture chamber system was designed to hold two coverslips in close proximity to each other. The device was drawn in Fusion360 (Autodesk Inc, CA, USA) and milled from 316L steel using a computer numerical controlled mill. The device consisted of two interlocking steel rings. A 24-mm diameter coverslip was placed at the base of the bottom ring on which one monoculture was established and submerged in medium in a cell culture dish. The second mono-culture was established on an 18-mm diameter coverslip, which was placed upside-down on a flange on the upper side of the bottom ring. The flange was 1-mm thick ensuring the coverslips were separated by this distance. The top ring was then positioned to complete the close-culture sandwich and ensure the upper coverslip was weighted in place for the duration of the experiment. Three access ports in the inner culture chamber, formed by the interconnected steel rings, facilitated medium exchange.

The bottom coverslip with astrocytes or microglia was exposed to 0.5  $\mu$ M  $\alpha$ SYN-F for 24h and thoroughly washed prior to the assembly of the chamber. A mixture of microglia and astrocyte medium (1:1) was added, and the untreated astrocytes/microglia coverslip was placed in the chamber upside down. The untreated cells (top coverslip) were co-cultured with  $\alpha$ SYN-F exposed cells (bottom coverslip) for 3d and then disassembled and fixed for analyses.

### Immunocytochemistry

Cells were fixed in 4% paraformaldehyde (PFA) (Sigma Aldrich) in PBS and washed twice with PBS. Blocking and permeabilization were performed with 5% normal goat serum (NGS) (Bionordika, S-1000) and 0.1% triton in PBS for 30 min in room temperature (RT). Primary antibodies were diluted in 0.5% NGS and 0.1% triton in PBS and added to the cells overnight (ON) at +4 °C. Thereafter, cells were washed 3 times with PBS prior to incubation with secondary antibodies or dyes for 1h at RT. After additional washes, the cells were mounted,

using Ever Brite Hardset Mounting medium with or without DAPI (BioNordika). Images were captured using a fluorescence microscope Observer and Z1 Zeiss. The primary antibodies used were chicken anti-vimentin antibody (Sigma Aldrich, AB5733), mouse anti-S100B antibody (Sigma Aldrich, S2532), Rabbit anti-ALDH1L1 (Novus biologicals, NBP2-24143), Chicken anti-GFAP (Abcam, ab4674), Rabbit anti-Iba1 antibody (Abcam, ab178846), Rabbit anti-P2Y12 antibody (Thermo Fisher, 702516), Mouse anti-CD68 (Abcam, ab955), and mouse anti-LAMP1 antibody (Abcam, ab25630). To stain the plasma membrane, cells were incubated with wheat germ agglutinin (WGA) Alexa Fluor® 350 Conjugate (Life technologies, 1:100) together with the primary antibodies ON. The secondary antibodies used were Alexa Flour 488 goat anti rabbit/mouse (Thermo Fisher, 1:200) and Alexa Flour 647 goat anti rabbit/mouse (Thermo Fisher, 1:200).

### Time-lapse microscopy

Cells were recorded using a time-lapse microscopy (Nikon Biostation IM Cell Recorder). Images were taken every 10 min with  $\times$ 20 and  $\times$ 40 objectives. The duration of the experiment was 24h+3days to 24h+6days.

### ELISA

EIA/RIA half area 96-well plates were used for all the ELISAs. Antibodies diluted in PBS were used for coating the plates ON at +4 °C. Then, the plates were blocked with 1% BSA in PBS at RT for 3h on shake at 900 rpm. ELISA incubation buffer (0.2% tween, 0.1% BSA, and 0.15% Kathon) was used to prepare standards, samples and antibody solutions, which were then added to the plates and incubated ON at 4 °C on shake (900 rpm). The next day, the plates were incubated with detection antibody for 2h at RT on shake and washed. The signal was developed using K-blue aqueous for 7 min, and 1M H<sub>2</sub>SO<sub>4</sub> was added to the plates to stop the reaction. Plates were read at 450nm using an Infinite M200 Pro.

### Total $\alpha$ SYN

For the  $\alpha$ SYN ELISA, MJFR1 (0.25 $\mu$ g/ml in PBS) (Abcam, 138501) was used as the coating antibody, and synthetic monomeric  $\alpha$ SYN (Proteos) was used as a standard for total  $\alpha$ SYN detection. Prior to analysis, the 0-time point medium samples (containing 0.5 $\mu$ M  $\alpha$ SYN-F) were diluted 1:50, the 24h time-point samples were diluted 1:10, and samples from the later time-points were left undiluted. Biotinylated anti- $\alpha$ SYN antibody clone 42 (BD Biosciences 610787, 0.35 $\mu$ g/ml) was used as detection antibody, followed by anti-mouse F(ab)<sub>2</sub>-HRP (1:2000, Jackson) incubation for 1h in RT on shake.

### Total A $\beta$

Anti-A $\beta_{42}$  antibody (Invitrogen 2 $\mu$ g/ml) was used as the coating antibody, and synthetic A $\beta_{42}$  was used as a standard. The medium samples, as well as the standards, were denatured in 0.5% sodium dodecyl sulfate (SDS) at 90 °C for 5min, followed by a 1:10 dilution (in order to lower the SDS concentration to 0.05% SDS). Biotinylated mAb4G8 (Nordic Biosite, 80070) was used as detection antibody, followed by incubation with SA-HRP (1:2000 Mabtech) for 1h at RT.

### Cytokine assay

Medium samples from astrocyte, microglia, and co-cultures were treated with  $\alpha$ SYN-F and A $\beta$ -F and collected and analyzed at 7d. Samples from microglia and astrocytes treated with 100ng/ml LPS for 24h was included as positive controls. The cytokine array (R&D systems, ARY005B) was performed according to the manufacturer's protocol. Shortly, the membranes were blocked with array buffer 4 at the same time as the samples were incubated with the detection antibody cocktail for 1 h on shake at RT. Next, the antibody-sample mixture was added to the membranes, which were incubated ON at 4 °C. The following day, the membranes were washed with the washing buffer 3  $\times$  10 min and incubated with HRP (1:1000) for 30 min before additional washes. The membranes were then incubated with a mixture of reagent 1 and 2 (1:1) for 10 min and developed in the chemiluminescent machine for 30s.

### Image analysis

#### Immunocytochemistry

The Z-layers of the  $\alpha$ SYN respective A $\beta$  channels were fused using ImageJ, and the mean integrated density (IntDen) (area\*mean intensity) was measured. In both the separate cultures and in the co-cultures, microglia and astrocytes were outlined using the cellular markers Iba1 and vimentin, limiting the analysis to internalized  $\alpha$ SYN/A $\beta$  only. The IntDen  $\alpha$ SYN/A $\beta$  signal was measured within the outlined cells. Since the astrocytes and microglia proliferated during the time course of the experiment (Supplementary Figure 1 and 2), we normalized the IntDen  $\alpha$ SYN/A $\beta$  signal to the area and not to the cell number. In proliferating cultures, normalization to the cell number is misleading as the deposits per cell will then be reduced without any degradation taking place.

#### Cytokine assay

An oval selection was generated as the region of interest. Mean intensity of each dot corresponding to a cytokine was measured using the oval selection. Medium samples from three independent experiments were analyzed.

### Statistical analysis

The level of significance for all the graphs was as follows: \* =  $P < 0.05$ , \*\* =  $P < 0.01$ , \*\*\* =  $P < 0.001$ , and \*\*\*\* =  $P < 0.0001$ .

### Image analysis

Sixty Z-stack images per time point and treatment for each culture system were captured from three independent experiments. The 4d, 7d, 24h+3d, and 24h+6d time points were normalized to the 24h time-point, and Kruskal-Wallis statistical analysis with Dunn's correction was performed as the groups failed to pass normality.

### $\alpha$ SYN and A $\beta$ measurements in ELISA

Medium samples from four different experiments were used for all ELISAs. The 0-time point was set to 100%, and all the other time points were normalized to the 0-time point, and one-way ANOVA with Tukey correction was performed.

## Results

### Astrocytes, but not microglia, accumulate $\alpha$ SYN-F over time

Human astrocytes, expressing the astrocytic markers vimentin, S100 $\beta$ , ALDH1L1 and GFAP (Supplementary Figure 3 A), and human microglia, expressing the microglial markers Iba1 and P2Y12 (Supplementary Figure 3 B) were derived from the same hiPSC line [27]. To compare the engulfment and accumulation of  $\alpha$ SYN-F by the astrocytes and microglia, the two cell types were cultured separately and exposed to  $\alpha$ SYN-F for 24h, 4d, and 7d (Fig. 1a). To be able to draw conclusions about the degradation capacity of the cells, parallel cultures were exposed to an  $\alpha$ SYN-F pulse and then cultured for additional time following removal of  $\alpha$ SYN-F from the medium (Fig. 1b). Already at 24h, Cy3-labelled intracellular  $\alpha$ SYN was detected in astrocytes, indicating uptake of  $\alpha$ SYN-F (Fig. 1c). Image analysis revealed that when the astrocytes were treated with  $\alpha$ SYN-F over the course of 7d, the intracellular  $\alpha$ SYN signal gradually increased (Fig. 1d). However, upon removal of extracellular  $\alpha$ SYN-F, the intracellular  $\alpha$ SYN signal decreased, indicating that the astrocytes were capable of degrading at least a proportion of the ingested  $\alpha$ SYN-F (Fig. 1e). Representative images of the  $\alpha$ SYN deposits in astrocytes at the different time points are shown in Fig. 1f. Similar to astrocytes, microglia showed a robust uptake of  $\alpha$ SYN-F at 24h (Fig. 1g). In contrast to the astrocytes, no increase was observed in the microglia cells over time. Instead, there was no significant change of intracellular  $\alpha$ SYN in the culture between the 24h and 7d time points (Fig. 1h). Upon extracellular  $\alpha$ SYN-F-removal, the intracellular  $\alpha$ SYN signal was dramatically reduced, indicating

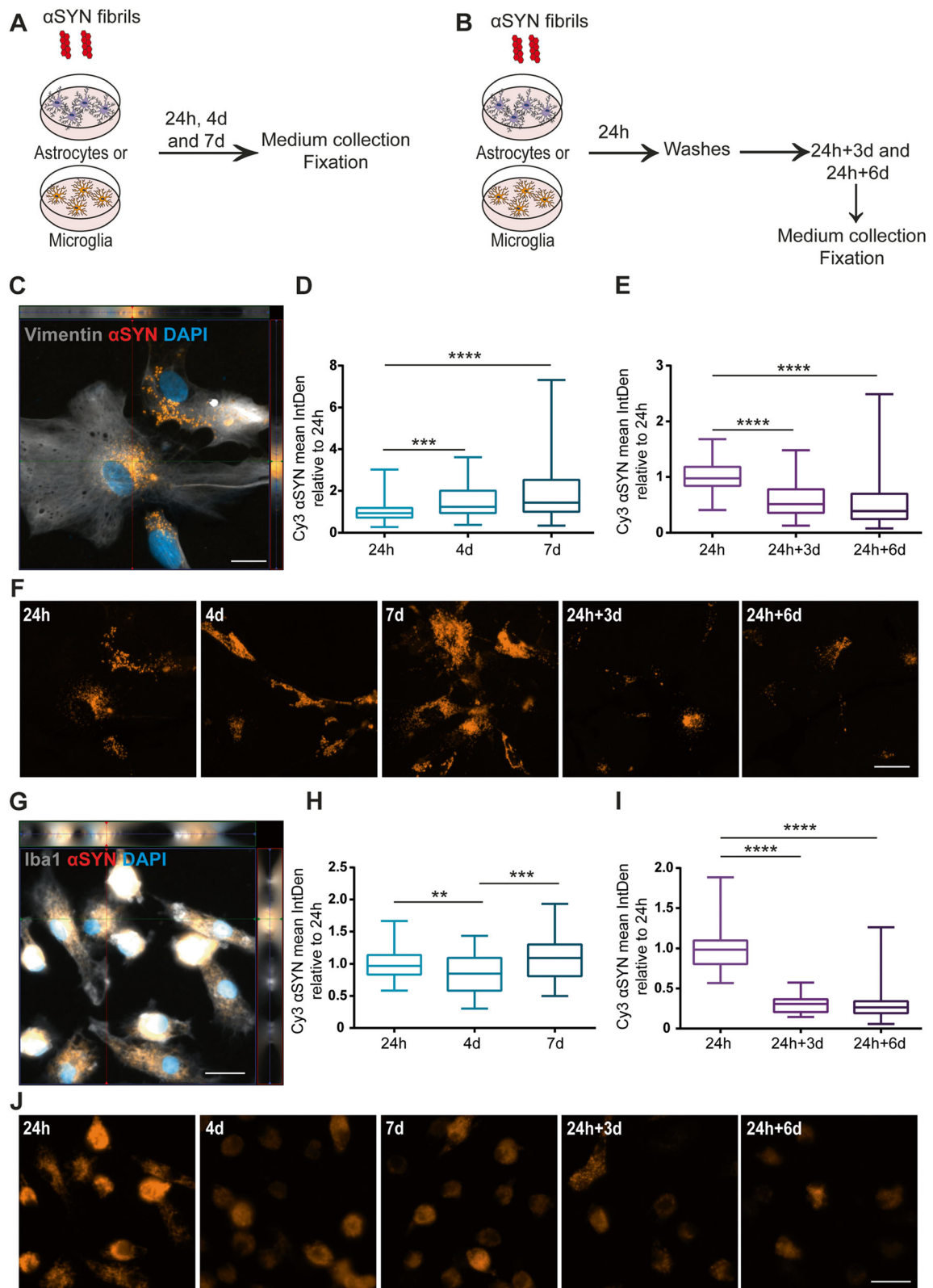


**Fig. 1** (See legend on next page.)

(See figure on previous page.)

**Fig. 1** In contrast to microglia, astrocytes accumulate  $\alpha$ SYN over time. Schematic figure of the study design illustrating that the cells were treated with  $\alpha$ SYN-F, either continuously (**a**) or with a 24h pulse (**b**). Astrocytes ingested and accumulated  $\alpha$ SYN-F already at 24h (**c**). However, the accumulation was continuous over the course of 7d, resulting in an increased intracellular signal of  $\alpha$ SYN (**d**). However, when the cells were washed at 24h and cultured without  $\alpha$ SYN-F for 3d and 6d, a significant reduction was observed over time (**e**). Representative images of the  $\alpha$ SYN deposits in astrocytes at the different time points are shown in **f**. Microglia showed extensive amounts of intracellular  $\alpha$ SYN-F at 24h (**g**). However, microglia did not show the same level of accumulation over time as compared to the astrocytes but had unchanged levels of intracellular  $\alpha$ SYN from 24h to 7d (**h**). Only low levels of  $\alpha$ SYN were present in microglia at 24h+3d and 24h+6d, indicating more effective degradation in microglia than in astrocytes (**i**). Representative images of the  $\alpha$ SYN deposits in microglia at the different time points are shown in (**j**). Scale bars = 20 $\mu$ m

that microglia are more effective than astrocytes when it comes to degrading the ingested  $\alpha$ SYN-F (Fig. 1i). Notably, intracellular  $\alpha$ SYN was still observed in both monocultures at 24h+6d, indicating that some deposits are more difficult for the cells to clear (Fig. 1e and i). Representative images of the  $\alpha$ SYN deposits in microglia at the different time points are shown in Fig. 1j. Since microglia continued to proliferate over the 7d, the  $\alpha$ SYN signal per cell was reduced over time, although the total  $\alpha$ SYN content in the culture was unchanged (Fig. 1h–j and Supplementary Figure 2).

#### Co-culturing of microglia and astrocytes results in reduced $\alpha$ SYN accumulation

Next, we investigated  $\alpha$ SYN-F uptake and accumulation in a microglia and astrocyte co-culture system. Similar to the monocultures, the co-cultures were either exposed to  $\alpha$ SYN-F continuously for 24h, 4d, and 7d (Fig. 2a) or received an  $\alpha$ SYN-F pulse (Fig. 2b). Using specific cell markers, we were able to analyze the intracellular  $\alpha$ SYN signal in the microglia and astrocytes, respectively (Fig. 2c). By normalizing  $\alpha$ SYN IntDen to the total number of respective cell type, we revealed that microglia cells contained significantly more  $\alpha$ SYN per cell at 24h and 4d, compared to the astrocytes (Fig. 2d and e and Supplementary Figure 4).

To find out if the co-existence of the two cell types affected the overall  $\alpha$ SYN accumulation, the total  $\alpha$ SYN signal in culture was analyzed. Interestingly, the total  $\alpha$ SYN signal was significantly reduced at 7d (Fig. 2f). This was in contradiction to the results in the monocultures, where  $\alpha$ SYN signal was increased at 7d in the astrocytes and unchanged in the microglia cultures (Fig. 1d and h). Hence, the presence of both microglia and astrocytes reduces the overall accumulation of  $\alpha$ SYN. To identify which cell type that was mainly responsible for the reduction, microglial and astrocytic  $\alpha$ SYN content was analyzed. Intracellular  $\alpha$ SYN signal appeared to be mostly reduced in astrocytes at 7d (Fig. 2g and h). In line

with the results from the monocultures, there was a clear reduction of intracellular deposits in the co-culture set-up, following removal of  $\alpha$ SYN (24h+3d and 24h+6d, Fig. 2i–k), although there were some remaining deposits that were not cleared.

#### Intracellular A $\beta$ levels remain stable in astrocytes, but decrease over time in microglia

Similar to the  $\alpha$ SYN-F experiments, monocultures of astrocytes and microglia were treated with A $\beta$ -F to study intracellular accumulation and degradation (Fig. 3a, b). The intracellular levels of A $\beta$ -F at 24h in astrocytes appeared lower than the levels of  $\alpha$ SYN-F (Fig. 3c). However, direct comparison of the Cy3-intensity could not be done, since the efficiency of Cy3-labelling of A $\beta$  and  $\alpha$ SYN may differ. Furthermore, no significant difference in intracellular A $\beta$  inclusions could be detected between 24h and 7d (Fig. 3d). At 4d+3d, the astrocytic A $\beta$  signal was slightly reduced, compared to the 4d time point, indicating that astrocytes were capable of degrading the ingested A $\beta$  to some degree (Fig. 3e). Representative images of the A $\beta$  deposits in astrocytes at the different time points are shown in Fig. 3f. The microglia cells showed an extensive uptake of A $\beta$ -F aggregates at 24h (Fig. 3g). In contrast to  $\alpha$ SYN, the intracellular A $\beta$  signal was significantly decreased at 4d. On the other hand, no change in intracellular A $\beta$  was observed from 4 to 7d (Fig. 3h). Although the intracellular A $\beta$  aggregates were significantly lowered at 24h+3d and 24h+6d, there were still some remaining A $\beta$  deposits at these time points, indicating that the microglia were not capable of complete degradation during the 6d time span (Fig. 3i). Representative images of the A $\beta$  deposits in microglia at the different time points are shown in Fig. 3j.

#### Astrocytes contain less A $\beta$ deposits when co-cultured with microglia

To examine whether culturing microglia and astrocytes together also decreased A $\beta$  accumulation, co-cultures were exposed to A $\beta$ -F continuously for 24h, 4d, and 7d

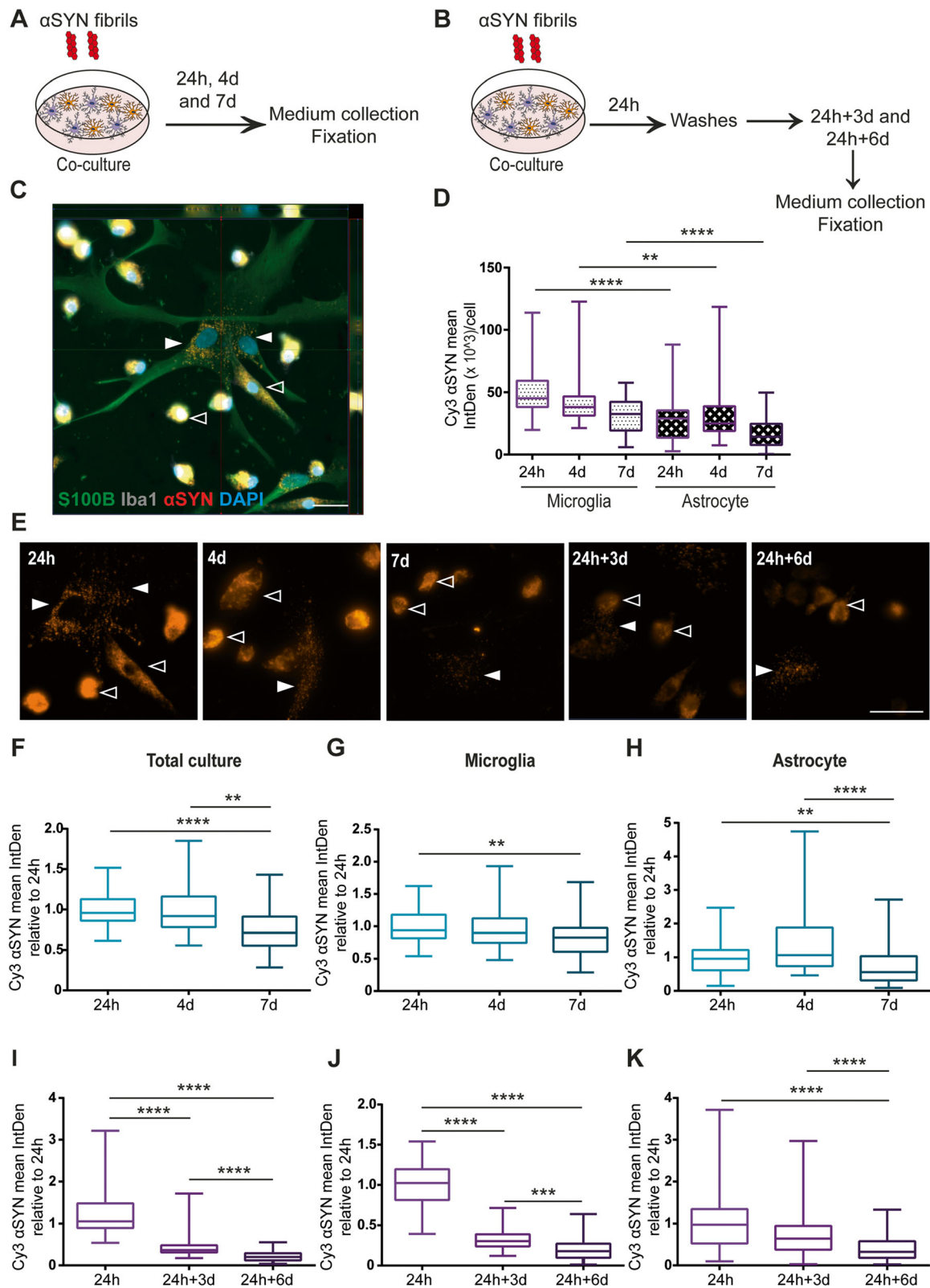


**Fig. 2** (See legend on next page.)



(See figure on previous page.)

**Fig. 2**  $\alpha$ SYN accumulation is reduced when microglia and astrocytes are co-cultured. Schematic figure of the study design illustrating that the cells were either treated with  $\alpha$ SYN-F constantly (a) or with a 24h pulse (b). Both astrocytes (Iba1- S100B+, filled arrow heads) and microglia (Iba1+, open arrow heads) ingested and accumulated  $\alpha$ SYN in the co-culture set-up (c). Image analysis showed that the microglia contained more  $\alpha$ SYN signal per cell at 24h and 4 d, compared to the astrocytes (d). Representative images of the  $\alpha$ SYN-F deposits at the different time points in the co-culture are shown in e; astrocytes and microglia are indicated with filled respective open arrow heads. Analysis of the total intracellular  $\alpha$ SYN in the co-culture revealed that there was an overall reduction of  $\alpha$ SYN at d7 in relation to the 24h time point (f). Separate image analysis of the  $\alpha$ SYN content in the two cell types of the co-culture confirmed that the decrease in  $\alpha$ SYN signal was significantly lower in both microglia (g) and astrocytes (h) at d7. For the astrocytes, the reduction in  $\alpha$ SYN was opposite to the pattern in the pure astrocytic culture, suggesting a lower accumulation of  $\alpha$ SYN within astrocytes in the co-culture. When the co-cultures were washed at 24h and cultured without  $\alpha$ SYN-F for 3d and 6d, a significant reduction was observed over time in the total co-culture (i), which was due to a decrease in both co-cultured microglia (j) and co-cultured astrocytes (k). Scale bars = 20 $\mu$ m

(Fig. 4a) or received an 24h A $\beta$ -F pulse (Fig. 4b). At 24h, both cell types had engulfed and accumulated A $\beta$ -F (Fig. 4c). Interestingly, in the co-culture set up, both cell types appeared to contain similar levels of A $\beta$  deposits (Fig. 4d and e and Supplementary Figure 5). This result was different from the monocultures, where microglia contained much more A $\beta$  than astrocytes (Fig. 3). At d7, the overall intracellular A $\beta$  signal in the co-culture had significantly decreased, compared to the 24h time point (Fig. 4f). To investigate which cell type was responsible for the reduction, microglial and astrocytic A $\beta$  were analyzed, respectively. At 7d, intracellular A $\beta$  levels were reduced in both microglia (Fig. 4g) and astrocytes (Fig. 4h), compared to 24h. This reduction in A $\beta$  deposits was not observed in the astrocytic monocultures (Fig. 3d). When we analyzed the cells that received an A $\beta$ -F pulse, we noted that the microglia cells contained more A $\beta$  inclusions at 24h+3d, compared to the astrocytes (Fig. 4i–k), indicating that the presence of microglia either increases the degradation capacity of the astrocytes or causes astrocytes to dispose of their inclusions via secretion or cell-to-cell transfer.

#### Microglia degrade aggregated $\alpha$ SYN and A $\beta$ better than astrocytes

Both the glial monocultures and co-cultures are heterogeneous, containing cells of various size and shape. We noted that in small cells, the inclusions were often more densely packed, while large cells displayed scattered deposits (Figs. 1, 2, 3, and 4). However, we were unable to identify cells with no intracellular deposits. In order to study how much of the  $\alpha$ SYN-F/A $\beta$ -F that were internalized by the two cell types, we next analyzed the conditioned medium at different time points, using ELISA. After 24h exposure, almost 75% of the added  $\alpha$ SYN had been cleared from the medium in all cell cultures, indicating that astrocytes and microglia are equally effective in ingesting  $\alpha$ SYN-F (Fig. 5a–c). Furthermore, the

$\alpha$ SYN levels were gradually reduced over 7d, suggesting that both astrocytes and microglia continuously take up new  $\alpha$ SYN-F independent of their intracellular  $\alpha$ SYN load. Together with the finding that intracellular  $\alpha$ SYN increased over time in astrocytes, but remained unchanged in microglia cells, our results suggest that microglia degrade  $\alpha$ SYN-F more effectively than astrocytes (at least when cultured separately). Interestingly, low but stable levels of  $\alpha$ SYN could be detected in the medium at 24h+3d and 24h+6d, indicating that the cells secrete some of their intracellular  $\alpha$ SYN into the medium (Fig. 5a–c).

Measurements of A $\beta$  levels in the medium (Fig. 5d–f) showed that astrocytes and microglia engulfed similar amounts of the A $\beta$ -F during the first 24h. However, while microglia cleared A $\beta$  from the medium also after the 24h, astrocytes showed no significant uptake of A $\beta$ -F between 24h to 7d, indicating that the intracellular A $\beta$  load affects their phagocytic capacity. At 4d + 3d, higher A $\beta$  levels were detected in the astrocyte medium compared to the microglia and the co-culture medium, suggesting that the astrocytes also secrete more A $\beta$  than the microglia (Fig. 5d–f).

Next, we analyzed the levels of various cytokines in the cell culture medium using a cytokine array (Supplementary Figure 6). Our data indicate that the exposure to aggregated  $\alpha$ SYN or A $\beta$  had very little effect on the cytokine profile.

#### Ingested $\alpha$ SYN enters the endo-lysosomal pathway and remains there

In our previous studies of human astrocytes, we have shown that  $\alpha$ SYN-F enters the endo-lysosomal pathway following ingestion [24]. To investigate if  $\alpha$ SYN-F and A $\beta$ -F also enters the endo-lysosomal pathway in microglia, the cells were stained for LAMP-1. By 24h, the majority of intracellular  $\alpha$ SYN/A $\beta$  were surrounded by LAMP-1 in both cell types (Fig. 6a–d). The pattern was identical in microglia and astrocytes cultured separately

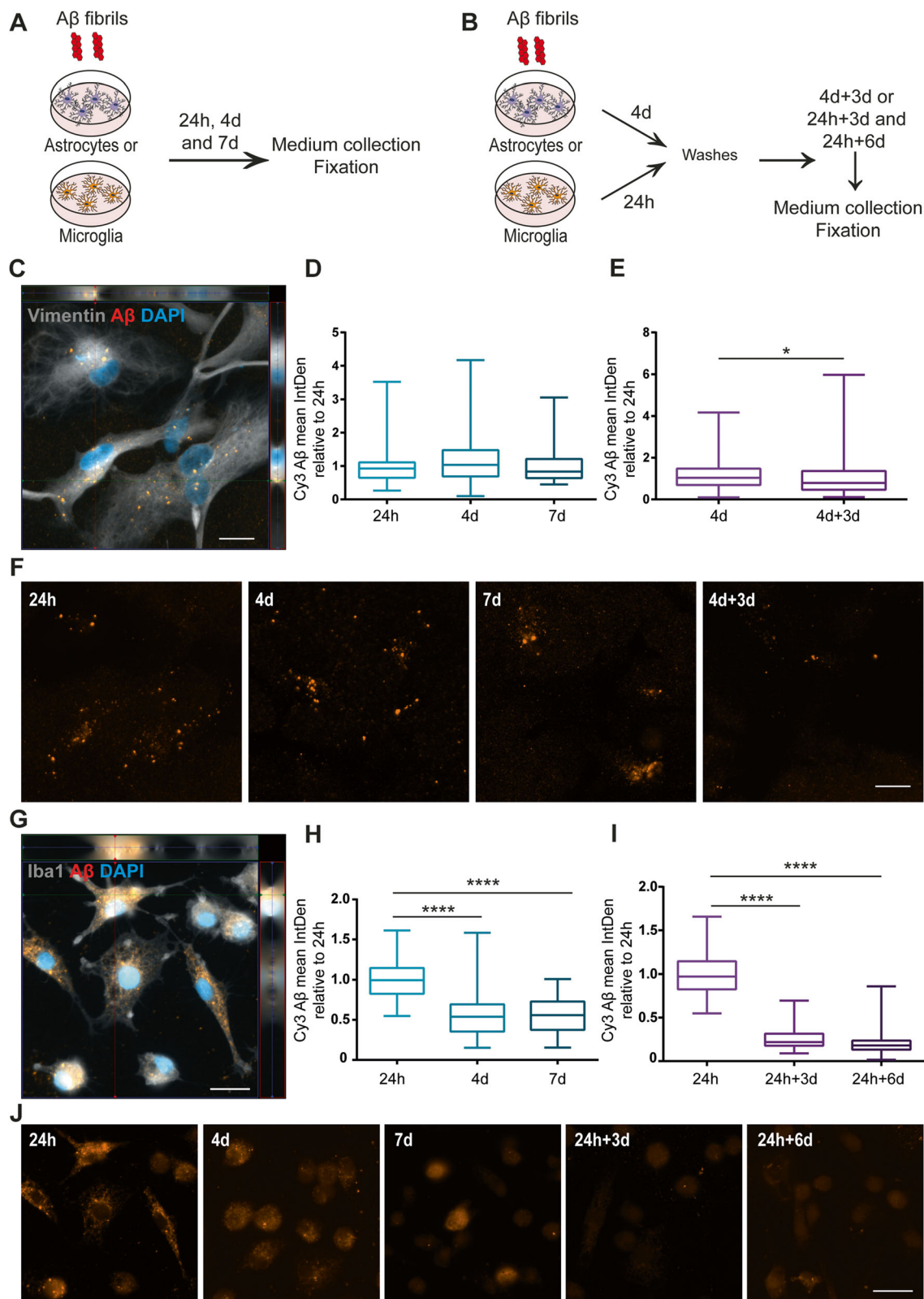


**Fig. 3** (See legend on next page.)

(See figure on previous page.)

**Fig. 3** Intracellular A $\beta$  levels are reduced in microglia over time but remain stable in astrocytes. Schematic figure of the study design illustrating that the cells were either constantly treated with A $\beta$ -F for 24h, 4d, and 7d (**a**) or treated with an A $\beta$ -F pulse (**b**), lasting for 24h (microglia) or 4d (astrocytes), followed by culture in A $\beta$ -F-free medium. Astrocytes had ingested and accumulated A $\beta$ -F already at 24h (**c**). The intracellular A $\beta$  accumulation was significantly increased after 4d compared to 24h (**d**). At 4d+3d, the astrocytic A $\beta$  signal was significantly reduced, compared to the 4d time point (**e**). Representative images of the A $\beta$  deposits in astrocytes at the different time points are shown in **f**. Large amounts of intracellular A $\beta$  could be detected in microglia at 24h (**g**). Contrary to the astrocytes, microglia showed a reduction in intracellular A $\beta$  signal at 4 days and 7d compared to 24h (**h**). Furthermore, the intracellular A $\beta$  aggregates in microglia were significantly lowered at 24h+3d and 24+6d, compared to 24h (**i**). Representative images of the A $\beta$  deposits in microglia at the different time points are shown in **j**. Scale bars = 20 $\mu$ m

or in co-culture. Furthermore, the protein aggregates remained in the lysosomal compartments at all-time points, regardless of cell type and culture system (Supplementary Figure 7), suggesting that the  $\alpha$ SYN-F/A $\beta$ -F is cleared predominantly by lysosomal degradation and do not end up in other cellular compartments. In addition to LAMP-1, the microglial cultures were stained for CD68, which showed a very similar expression pattern. No change in the intensity of the CD68 staining was detected following  $\alpha$ SYN or A $\beta$  exposure (Supplementary Fig 8).

#### Astrocytes transfer $\alpha$ SYN aggregates to microglia via secretory mechanisms

The observed reduction in astrocytic  $\alpha$ SYN, when co-cultured with microglia, raised the possibility of active transfer of  $\alpha$ SYN between the glia populations either via a secretion and uptake pathway or through direct cell-to-cell contact. Accordingly, we first performed conditioned media experiments (Fig. 7a, b). We observed that microglia internalized large amounts of  $\alpha$ SYN, when treated with conditioned medium from  $\alpha$ SYN-exposed astrocytes (Fig. 7c, d). In contrast, astrocytes treated with conditioned media from  $\alpha$ SYN-exposed microglia had very low levels of intracellular  $\alpha$ SYN (Fig. 7d). To further verify the diverse spreading of  $\alpha$ SYN from astrocytes to microglia and vice versa, we performed experiments with a customized “close-culture” cell chamber (Supplementary Figure 9), in which the apical surfaces of astrocyte and microglia monocultures were separated by a <1 mm space. This space served as a common medium reservoir, which permitted the paracrine exchange of material, but prevented direct contact between the different cell-types (Fig. 7e, f). Our results confirm that astrocytes transfer a large proportion of their intracellular  $\alpha$ SYN to microglia via secretory mechanisms, while microglia hardly transfer any  $\alpha$ SYN to the astrocytes (Fig. 7g, h).

#### Extensive contact between astrocytes and microglia enable cell-to-cell transfer of aggregated $\alpha$ SYN

Subsequently, we analyzed whether the astrocytes and microglia are in direct contact, as this could be another

potential mechanism to spread  $\alpha$ SYN from one cell to another. Indeed, multiple TNTs were formed between the astrocytes and microglia in the co-culture (Fig. 8a, b). Notably, deposits of aggregated  $\alpha$ SYN could be found within the TNTs, indicating TNT-mediated transfer (Fig. 8c, d). We also observed frequent membrane contact between astrocytes and microglia (Fig. 8e). Often, the microglial cells were found within a ring-shaped area, completely surrounded by an astrocytic membrane. These microglia contacted the surrounding astrocyte with sprouting extensions (Fig. 8f). Live cell imaging shed further light on the complex crosstalk between astrocytes and microglia (Fig. 9a). We noticed that large  $\alpha$ SYN-containing vesicles that were secreted from the astrocytes were effectively removed by the patrolling microglia (Fig. 9b). As previously, we found microglial cells encircled by astrocytic membranes (Fig. 9c), and in contact with the surrounding astrocyte via sprouting extensions (Fig. 9c). Interestingly, whenever this cellular arrangement occurred, the  $\alpha$ SYN deposits in the astrocytes, which was prominently located around the nucleus, was shifted to the side of the interacting microglia (Fig. 9c). We also noted that the  $\alpha$ SYN load in the astrocyte was dramatically reduced during the microglia interaction, indicating that microglia attract and clear intracellular protein deposits directly from the astrocytes (Fig. 9c).

#### Discussion

Growing evidence indicates that insufficient degradation of protein aggregates and chronic inflammation are driving forces of AD and PD brain pathology [30–32]. Consequently, the role of glial cells in disease progression has received much attention lately. Microglia and astrocytes are known to be responsible for many inflammatory processes in affected brains, including phagocytosis of  $\alpha$ SYN and A $\beta$  aggregates, secretion of inflammatory mediators, and stimulation of the innate immune system [8–12]. In order to develop effective therapies, it is of great importance to understand how the two glial cell types communicate and coordinate their responses to  $\alpha$ SYN and A $\beta$

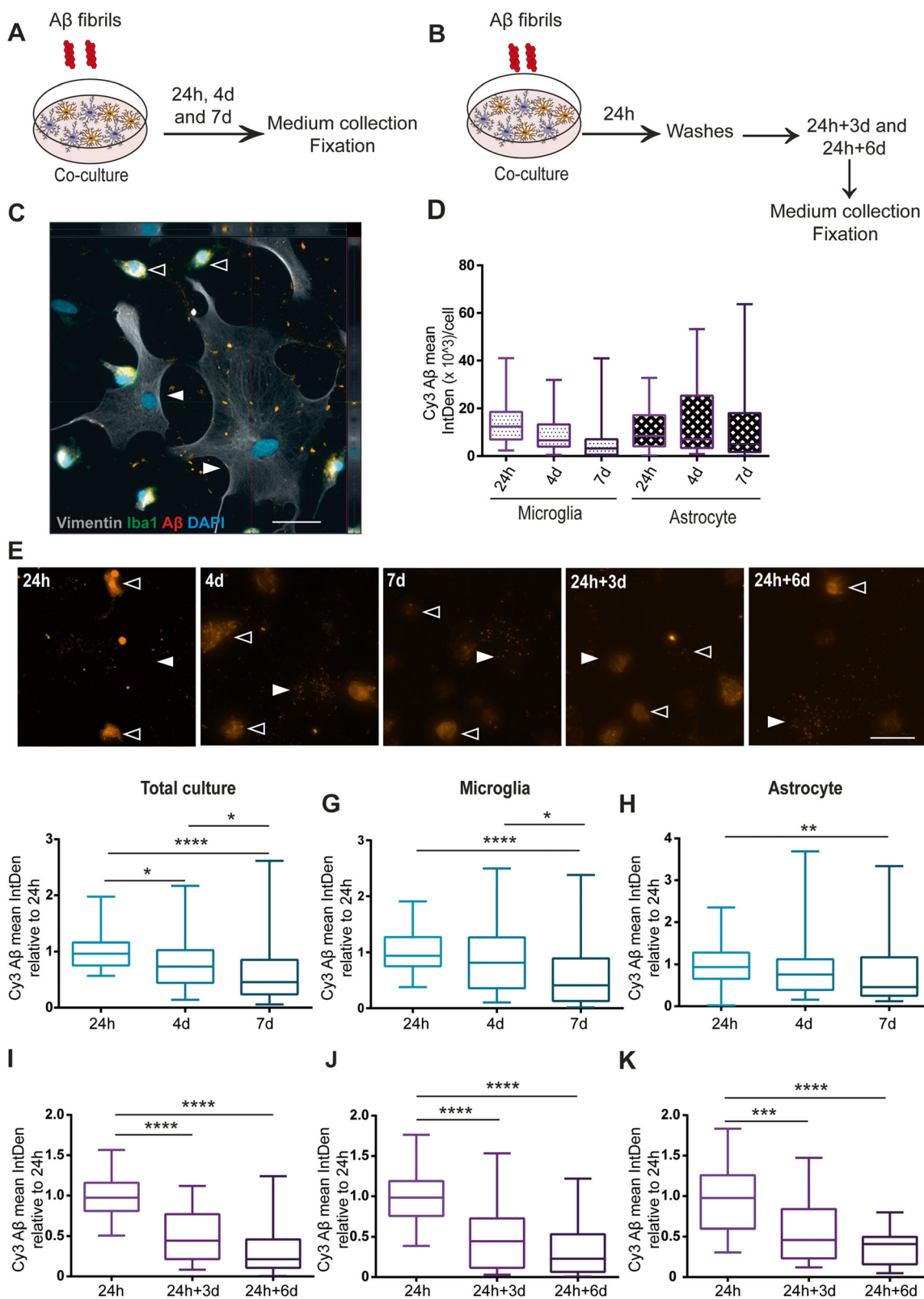


**Fig. 4** (See legend on next page.)

(See figure on previous page.)

**Fig. 4** Intracellular Aβ is reduced when astrocytes and microglia are cultured together. Schematic figure of the study design illustrating that the cells were either treated with Aβ-F constantly (a) or with a 24h Aβ-F pulse (b). In the co-culture, both astrocytes (Iba1- S100B+, filled arrow heads) and microglia (Iba1+, open arrow heads) ingested and accumulated Aβ-F (c). Image analysis and normalization to the number of cells confirmed that astrocytes and microglia contained comparable levels of Aβ at 24h, 4d and 7d (d). Representative images of the Aβ deposits at the different time points in the co-culture are shown in (e); astrocytes and microglia are indicated with filled respective open arrow heads. Analysis of the total intracellular Aβ in the co-culture revealed that intracellular Aβ was lower in the culture at 7d, compared to 24h (f). Separate analysis of the two cell types in the co-culture demonstrated that the astrocytes, rather than the microglia, were responsible for this reduction (g, h). When the co-cultures were washed at 24h and cultured without Aβ-F for 3d and 6d, a significant reduction was observed over time (i), which was due to a decrease in both microglia (j) and astrocytes (k). Scale bars = 20μm

pathology. We have previously shown that astrocytes accumulate large amounts of αSYN and Aβ aggregates, resulting in severe cellular stress [11, 12, 23, 24]. The aim of the present study was to compare uptake and accumulation of αSYN and Aβ in human astrocytes and microglia, when cultured separately or

in a co-culture set up. Moreover, we sought to identify specific mechanisms by which the two cell types crosstalk in regard to αSYN and Aβ pathology.

Our data show that in the separate cultures, both microglia and astrocytes ingest αSYN and Aβ aggregates, but microglia appear to be more effective in degrading

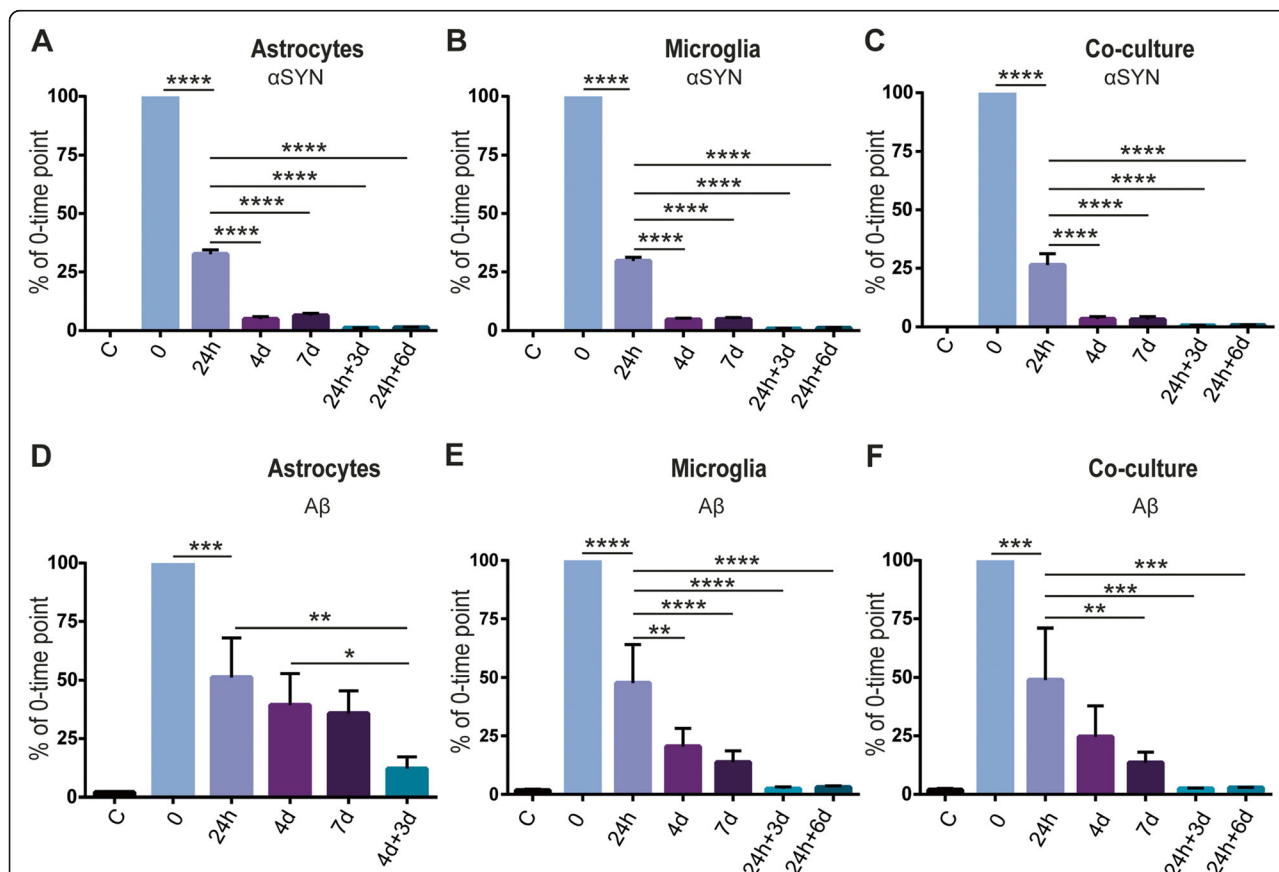


**Fig. 5** Astrocytes and microglia clear equal amounts of αSYN, but microglia clear extracellular Aβ more effectively. αSYN levels in the medium revealed that both astrocytes and microglia engulfed almost 75% of the initial αSYN. Furthermore, both astrocytes and microglia continued to ingest αSYN during the 7d of exposure. Secretion of αSYN was observed in all cultures at 24h+3d and 24h+6d (a-c). Analysis of Aβ in the medium revealed that astrocytes were less efficient in engulfing Aβ, compared to microglia. In the co-culture set-up, cells engulfed Aβ at the same level as in the microglial culture. Also, low secretion of Aβ could be observed at 24h+3d and 24h+6d in the microglia and co-cultures, whereas higher Aβ levels was observed at 4d+3d in the astrocyte cultures (d-f)

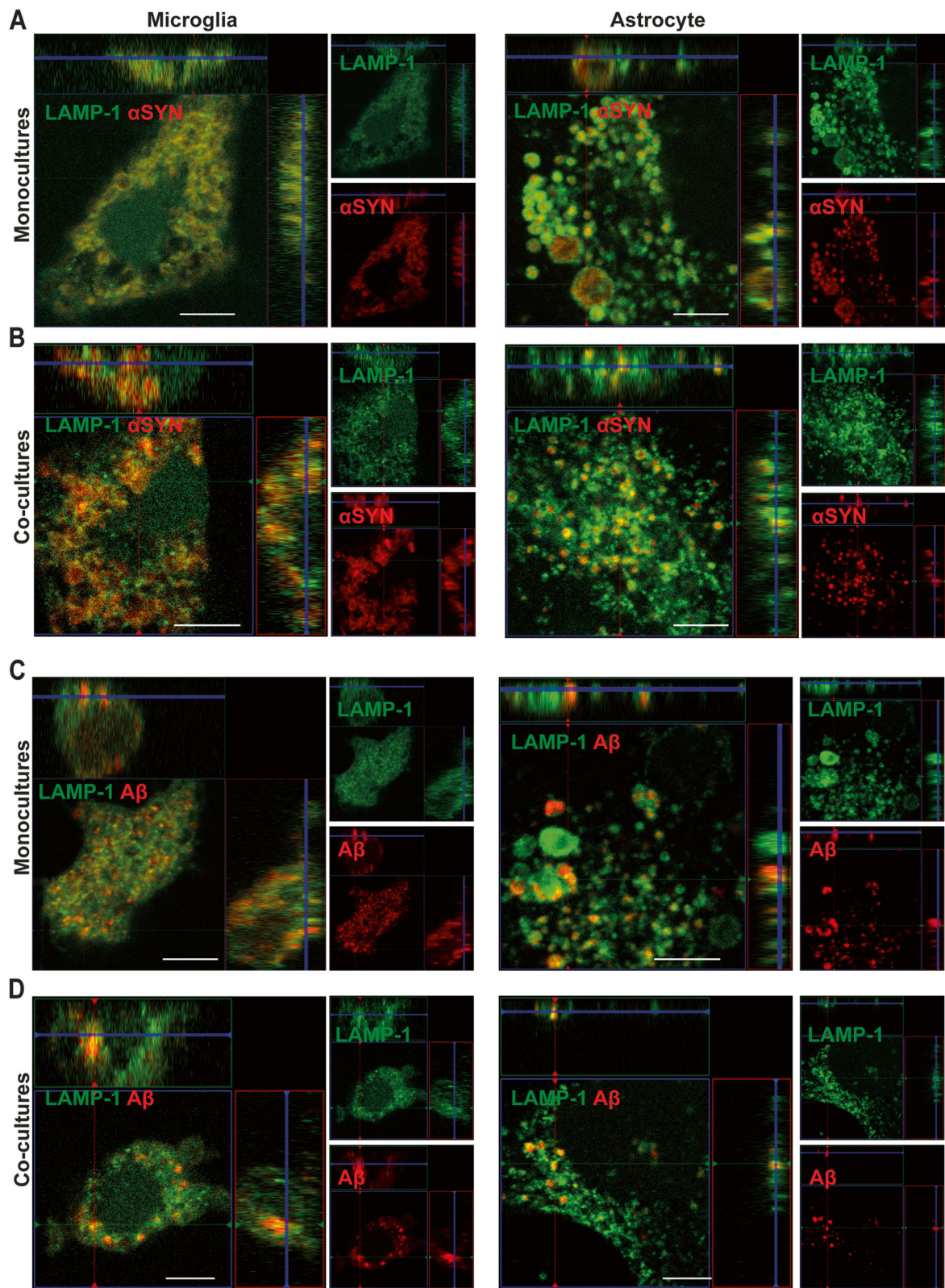


**Fig. 6** Ingested  $\alpha$ SYN-F and  $A\beta$ -F are located in LAMP1+ vesicles. Confocal microscopy demonstrated that intracellular deposits of  $\alpha$ SYN (**a, b**) and  $A\beta$  (**c, d**) were surrounded by LAMP1+ vesicles in both monocultures of astrocytes and microglia (**a** and **c**) and in the co-cultures (**b** and **d**). Scale bars = 20 $\mu$ m

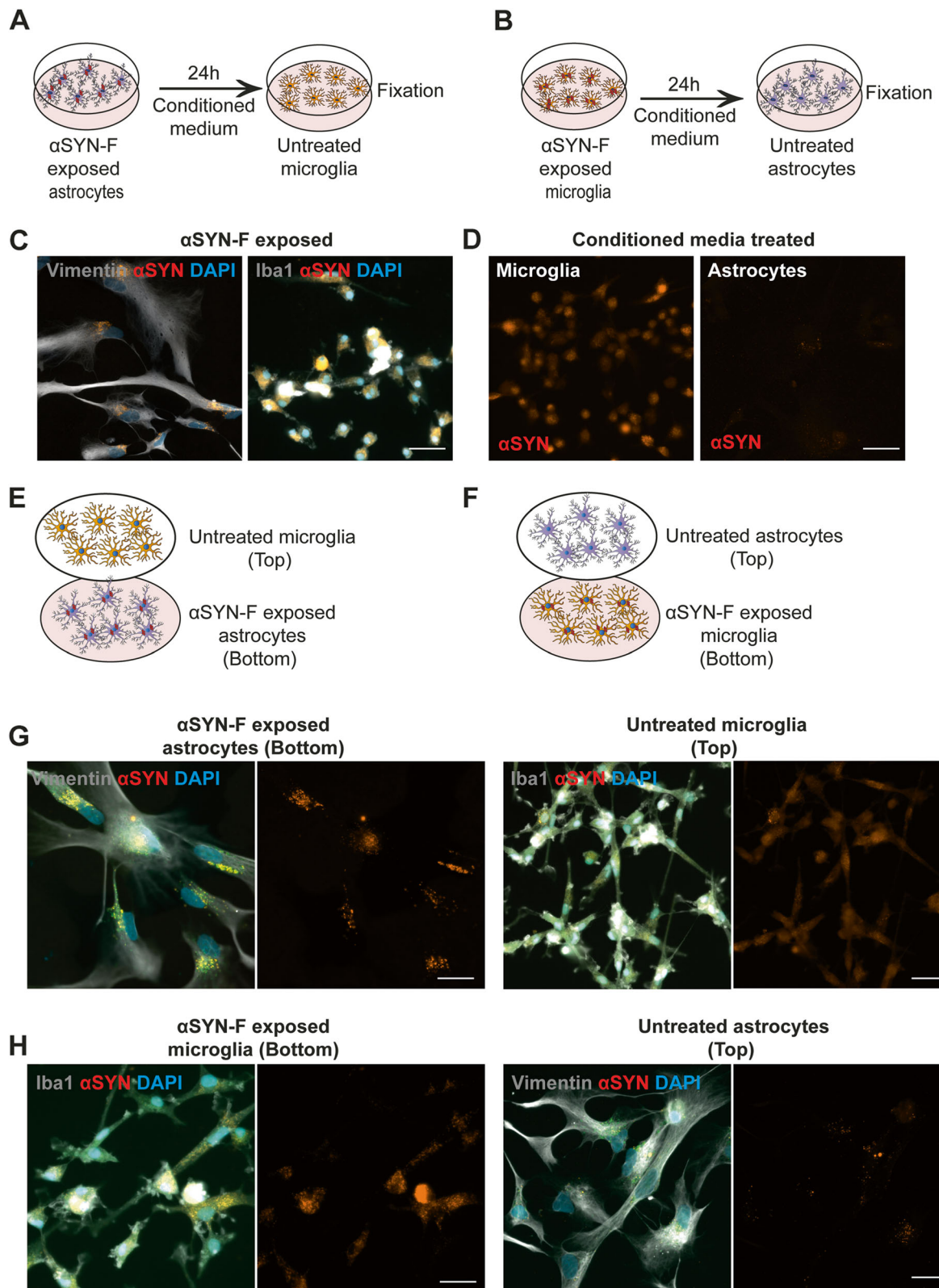


**Fig. 7** (See legend on next page.)

(See figure on previous page.)

**Fig. 7** Secreted  $\alpha$ SYN aggregates are transferred from astrocytes to microglia. Conditioned media experiments were performed to investigate if transfer of  $\alpha$ SYN occurred from one cell type to another via secretion (**a, b**). Microglia that received conditioned medium from  $\alpha$ SYN-exposed astrocytes contained high levels of  $\alpha$ SYN, while astrocytes that received microglia medium had very little intracellular  $\alpha$ SYN (**c, d**). To further study secretory spreading of  $\alpha$ SYN aggregates between the two cell types, we performed experiments using a customized close-culture chamber, in which the astrocytes and microglia were cultured face-to-face, separated by a <1-mm space. In the chamber, either untreated microglia were co-cultured with  $\alpha$ SYN-exposed astrocytes (**e**) or untreated astrocytes were co-cultured with  $\alpha$ SYN-exposed microglia (**f**). Consistently with the conditioned media data, astrocytes were found to transfer a large proportion of their internalized  $\alpha$ SYN to microglia (**g**), while microglia hardly transferred any  $\alpha$ SYN to the astrocytes (**h**). Scale bars = 20 $\mu$ m

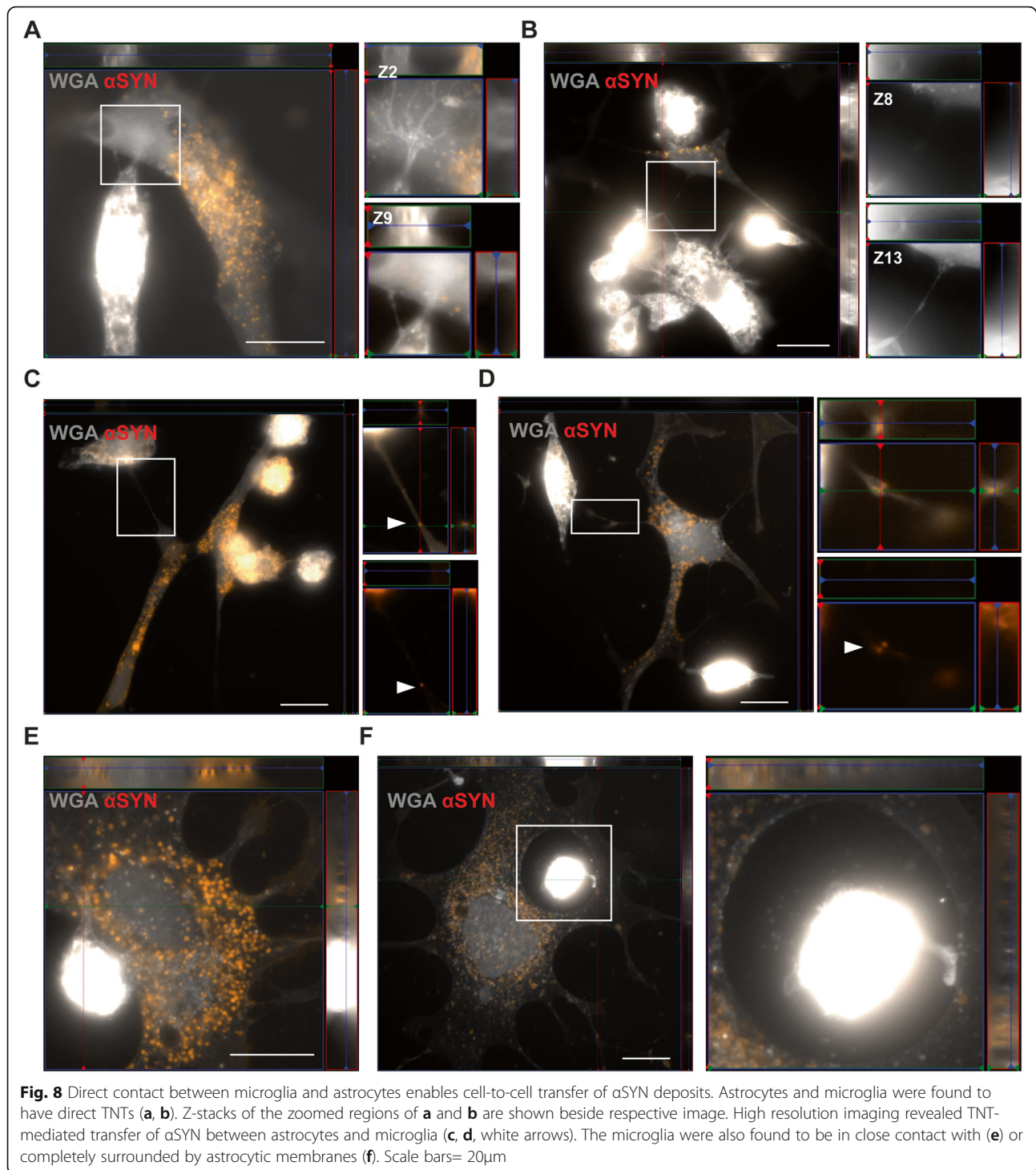
the protein aggregates. In a recent publication, we showed that astrocytes, but not microglia, have the capacity to act as antigen-presenting cells (APCs) when exposed to  $\alpha$ SYN fibrils [24]. Accordingly, astrocytes could be found in very close proximity to infiltrating T cells in the PD brain [24]. One of the features of APCs is the ability to degrade antigens slowly in order to present them on the surface for T cells. These observations gave rise to the idea that microglia may be primarily responsible for degrading protein aggregates, whereas astrocytes may act as a bridge between the brain and the peripheral immune system. This idea has further support from the fact that astrocytes are essential for the formation and maintenance of the blood-brain barrier.

In our co-culture experiments, we could observe that, even though both cell types engulfed  $\alpha$ SYN and A $\beta$  fibrils, microglia were responsible for a greater uptake of the aggregates. Interestingly, astrocytes accumulated less  $\alpha$ SYN and A $\beta$  deposits in the co-cultures, compared to the monocultures. A recent study showed that astrocytes and microglia degrade dead cells in a very organized and specialized manner; microglia degrade neuronal dendrites, cell bodies, and nuclei while astrocytes phagocytose apoptotic bodies that are released from the dying neurons [10]. These data suggest that microglia and astrocytes could share the burden by dividing toxic materials in a size-dependent manner, where microglia would phagocytose bigger aggregates and astrocytes smaller aggregates. These observations are in line with our previous discoveries that astrocytes easily degrade  $\alpha$ SYN and A $\beta$  monomers, while they accumulate larger oligomers and fibrils [11, 12]. Hence, it is possible that astrocytes engulf less protein aggregates in the presence of microglia and thereby allow better degradation of the ingested material. Damisah et al. provide support for this in their recent study, where microglia were eliminated from mice using a CSF1R antagonists, after which neuronal cell death was induced. They found that astrocytes engulfed the material which was intended for microglia but degraded it at a slower rate [10]. An accumulating body of evidence emphasizes astrocytes as one of the major

secretory cells in the CNS, responsible for secretion of neurotransmitters, growth factors, inflammatory mediators, and toxic proteins [33]. We have previously shown that an incomplete degradation of A $\beta$ <sub>42</sub> protofibrils by astrocytes results in the release of extracellular vesicles containing N-truncated, neurotoxic A $\beta$  [12]. Here, we observed that microglia phagocytosed large amounts of  $\alpha$ SYN from astrocytic conditioned medium, whereas very little  $\alpha$ SYN could be detected in astrocytes that had been treated with microglial-conditioned medium. Based on these results and previous studies, we hypothesize that astrocytes secrete some of the ingested  $\alpha$ SYN and A $\beta$ , which is then phagocytosed by the surrounding microglia. Several studies have demonstrated that astrocytes are capable of stimulating microglia phagocytosis by secretion of cytokines such as IL33 and the complement protein C3 [19, 34]. Therefore, investigating what inflammatory molecules astrocytes and microglia secrete when co-cultured would provide valuable insights into how they crosstalk.

Our previous results indicate that astrocytes are capable of transferring  $\alpha$ SYN as well as MHCII to other astrocytes via direct membrane contact and through TNTs, implicating astrocytes as one of the important players in propagation of  $\alpha$ SYN pathology [11, 24]. In the co-culture experiments in this study, we found that astrocytes also establish direct contact with microglia and that the two glial cell types remained in a continual alliance for a long time, as shown by immunocytochemistry and time-lapse microscopy. Notably, we could for the first time show that astrocytes and microglia are frequently connected via TNTs. The presence of  $\alpha$ SYN deposits within the TNTs suggest that these structures are used for cell-to-cell transfer of protein aggregates. Moreover, microglia were often situated in ring-shaped areas, “in the middle” of astrocytes, clearly anchored to the astrocyte membrane via extending protrusions. As shown with our time-lapse recordings, the  $\alpha$ SYN-deposits appeared to be immediately degraded, after being transferred from astrocytes to microglia. These findings are intriguing, but further studies using for



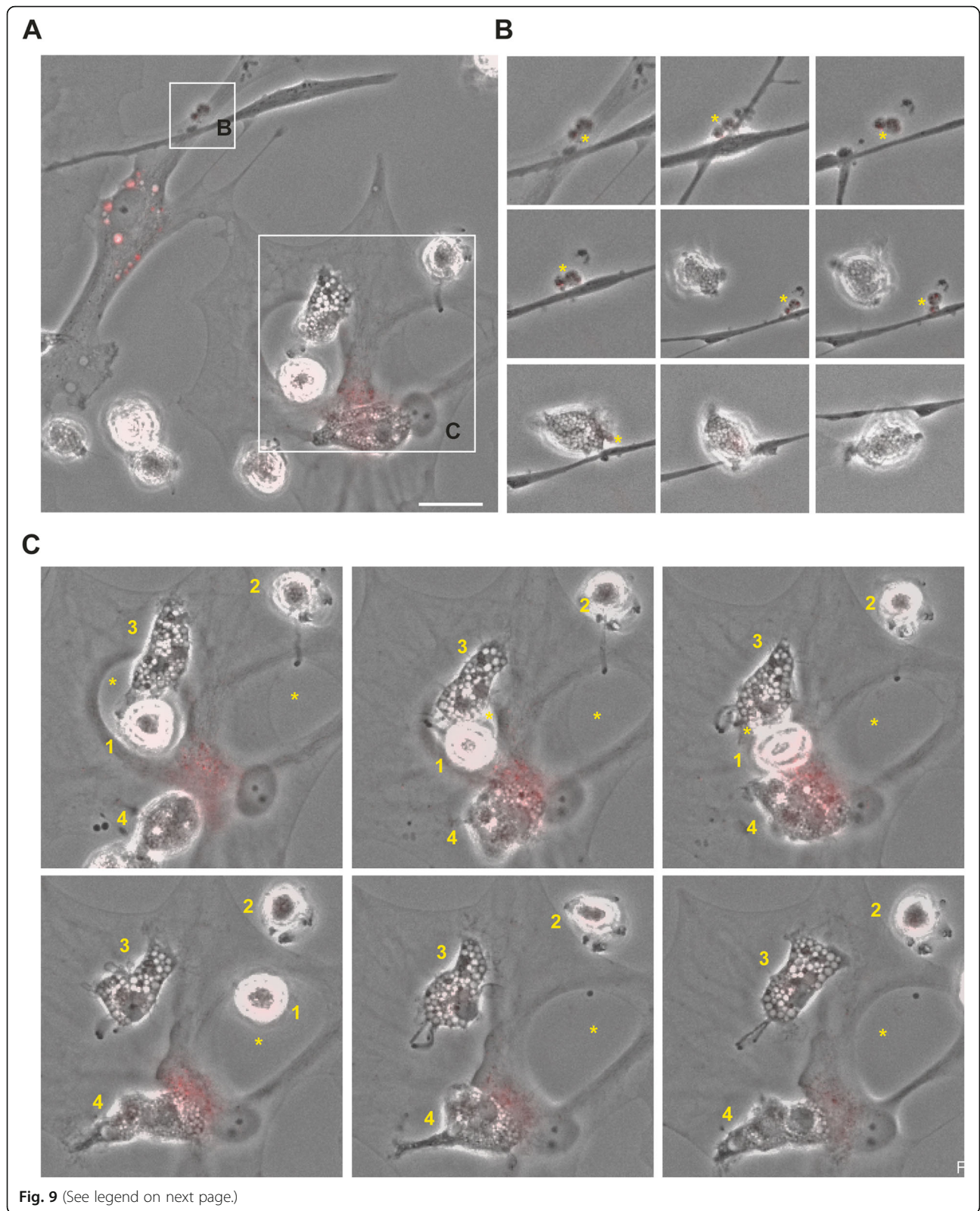


example multi-photon microscopy are needed to confirm the phenomenon in the living brain.

### Conclusions

In conclusion, our results demonstrate that there is a synergistic effect of astrocytes and microglia in

processing of  $A\beta$  and  $\alpha$ SYN aggregates, with relevance to AD and PD pathogenesis. Mainly, this interplay between the two cell types involves transfer of protein aggregates from astrocytes to microglia, which may be an important mechanism for the clearance of protein aggregates within affected brains. However, it may also



(See figure on previous page.)

**Fig. 9** Microglia can attract and clear intracellular  $\alpha$ SYN deposits from astrocytes via membrane contact. Time-lapse microscopy illustrated a complex interplay between astrocytes and microglia (**a**). Different time points of the regions of interest are shown in **b** and **c**. For **b**, the total duration from the first to last image is 10h and for **c** 11h. Astrocytes secreted large  $\alpha$ SYN-containing vesicles (yellow star) that were ingested by microglia (**b**). Moreover, microglia were found to be in direct contact with astrocytes in ring-shaped areas (yellow star) encapsulated by astrocytic membrane (microglia 1) or attached to the cell membrane of this area (microglia 2) (**c**). Microglia were anchored to the astrocyte membrane via distinct protrusions (microglia 2 and 3) and often interacted with the astrocytes in the region where the most intracellular  $\alpha$ SYN deposits were situated (microglia 4). During this interaction, the deposits appeared to decrease dramatically, indicating direct  $\alpha$ SYN transmission followed by instant degradation. Scale bar= 10 $\mu$ m

constitute a risk for spreading the pathology within and between interconnected networks. Taken together, our results highlight the importance of microglia-astrocyte crosstalk with respect to AD and PD pathology. Apart from increasing our knowledge on the underlying disease mechanisms, these insights may be of great relevance for identifying new therapeutic targets for these neurodegenerative disorders.

#### Abbreviations

$\alpha$ SYN : Alpha-synuclein;  $\alpha$ SYN-F: Alpha-synuclein fibrils; AD: Alzheimer's disease; A $\beta$ : Amyloid-beta; A $\beta$ -F: Amyloid-beta fibrils; APC: Antigen-presenting cells; bFGF: Basic fibroblast growth factor; CNTF: Ciliary neurotrophic factor; IGF-1: Insulin-like growth factor 1; HPC: Hematopoietic stem cell; iPSCs: Induced pluripotent stem cells; NES: Neuroepithelial-like stem cells; PD: Parkinson's disease; TNT: Tunneling nanotubes

## Supplementary Information

The online version contains supplementary material available at <https://doi.org/10.1186/s12974-021-02158-3>.

**Additional file 1:** Supplementary Figure 1. Astrocytes proliferate during the time course of the experiment. Quantification of the number of viable cells per field demonstrated that the astrocytes proliferate during the 7d period.

**Additional file 2:** Supplementary Figure 2. Microglia proliferate during the time course of the experiment. Quantification of the number of viable cells per field demonstrated that the microglia proliferate during the 7d period.

**Additional file 3:** Supplementary Figure 3. Characterization of astrocyte and microglia cultures. Human iPSC derived astrocytes expressed the astrocytic markers GFAP, ALDH1L1, vimentin and S100 $\beta$  (A). Human iPSC derived microglia expressed Iba1 and P2Y12 (B).

**Additional file 4:** Supplementary Figure 4.  $\alpha$ SYN accumulation is reduced when microglia and astrocytes are co-cultured. The separate channels from Figure 2E. Scale bar = 20  $\mu$ m.

**Additional file 5:** Supplementary Figure 5. Intracellular A $\beta$  is reduced when astrocytes and microglia are cultured together. The separate channels from Figure 4E. Scale bar = 20  $\mu$ m.

**Additional file 6:** Supplementary Figure 6. Unchanged cytokine profile following  $\alpha$ SYN or A $\beta$  exposure. Cytokine array data indicate that exposure to aggregated  $\alpha$ SYN or A $\beta$  had very little effect on the cytokine profile of astrocytes and microglia, both in monocultures and in co-cultures. Measurements of three independent experiments did not reveal any significant differences between the cultures.

**Additional file 7:** Supplementary Figure 7. Ingested  $\alpha$ SYN is located in LAMP1+ vesicles. Intracellular deposits of  $\alpha$ SYN was surrounded by LAMP1+ vesicles at all-time points in both separate cultures of astrocytes

(A) and microglia (B) and in co-cultures (C). Close-up images of the white rectangles are shown below. Scale bars = 20 $\mu$ m.

**Additional file 8:** Supplementary Figure 8. Expression of CD68 in microglia following  $\alpha$ SYN or A $\beta$  exposure. The myeloid-specific endo-lysosomal marker, CD68, was expressed by the microglia. No change in the intensity of the CD68 staining was detected over time or following  $\alpha$ SYN or A $\beta$  exposure. Scale bars = 20 $\mu$ m.

**Additional file 9:** Supplementary Figure 9. Close-culture chamber device. Exploded view of the close-culture chamber system consisting of interlocking top and bottom steel rings, and two coverslips (A). Top view of the assembled close-culture chamber, indicating the position of 3 access ports, which facilitate medium exchange, and the outer (32 mm) and inner (15 mm) diameters of the rings (B). Cross-sectional cutaway view of the assembled close-culture chamber. The enlarged area illustrates the width (1.75 mm) of the flange on which the upper coverslip rests, and the 1 mm open space between the sandwiched coverslips (C). Monocultures are established on each of the coverslips, and when assembled in the device the apical surfaces of cell-type 1 (e.g. astrocytes) and cell-type 2 (e.g. microglia) are separated by a gap of < 1 mm, but share a common reservoir of growth medium (D).

#### Acknowledgements

CAD design was performed at U-PRINT: Uppsala University's 3D-printing facility at the Disciplinary Domain of Medicine and Pharmacy. We thank the iPS Core at Karolinska Institutet.

#### Authors' contributions

JR designed the study, optimized and performed experiments, interpreted data, and wrote the manuscript; TM performed experiments, interpreted data, and wrote the manuscript; MK optimized microglia culture protocols and wrote the manuscript; OE designed the close-culture chamber and wrote the manuscript; MM optimized cell culture protocols, produced the NES cells, and wrote the manuscript; JB interpreted data and wrote the manuscript; MI interpreted data and wrote the manuscript; POC designed the close-culture chamber, interpreted data, and wrote the manuscript; LMH optimized microglia culture protocols, interpreted data, and wrote the manuscript; AF optimized cell culture protocols, coordinated the NES cell production, interpreted data, and wrote the manuscript; AE designed the study, interpreted data, coordinated the study, and wrote the manuscript. The authors have read and approved the final manuscript.

#### Funding

This study was supported by grants from the Swedish Research Council, the Swedish Parkinson Foundation, the Swedish Alzheimer Foundation, the Swedish Brain Foundation, Åhlén Foundation, the Dementia Association Foundation, Torsten Söderberg Foundation, O and E Edla Johanssons Foundation, Olle Engkvist Byggmästare Foundation, Bertil and Ebon Norlin Foundation, and Stohnes Foundation.

#### Availability of data and materials

All data used and analyzed for the current study are available from the corresponding author on reasonable request.

## Declarations

### Ethics approval and consent to participate

Not applicable.

### Consent for publication

All authors have given their consent for publication.

### Competing interests

The authors declare that they have no competing interests.

### Author details

<sup>1</sup>Molecular Geriatrics, Rudbeck Laboratory, Department of Public Health & Caring Sciences/, Uppsala University, Uppsala, Sweden. <sup>2</sup>Department of Neurology and Neurosurgery, Montreal Neurological Institute, McGill University, Montreal, Canada. <sup>3</sup>Department of Medical Cell Biology, Uppsala University, Uppsala, Sweden. <sup>4</sup>Department of Neuroscience, Karolinska Institutet, Stockholm, Sweden.

Received: 15 January 2021 Accepted: 23 April 2021

Published online: 03 June 2021

## References

- Matejuk A, Ransohoff RM. Crosstalk between astrocytes and microglia: an overview. *Frontiers in Immunology*. 2020;11:1416. <https://doi.org/10.3389/fimmu.2020.01416>.
- Goedert M. Parkinson's disease and other alpha-synucleinopathies. *Clin Chem Lab Med*. 2001;39(4):308–12. <https://doi.org/10.1515/CCLM.2001.047>.
- LaFerla FM, Green KN, Oddo S. Intracellular amyloid-beta in Alzheimer's disease. *Nat Rev Neurosci*. 2007;8(7):499–509. <https://doi.org/10.1038/nrn2168>.
- Mayne K, White JA, McMurrin CE, Rivera FJ, de la Fuente AG. Aging and neurodegenerative disease: is the adaptive immune system a friend or foe? *Front Aging Neurosci*. 2020;12:572090. <https://doi.org/10.3389/fnagi.2020.572090>.
- Allen NJ, Eroglu C. Cell biology of astrocyte-synapse interactions. *Neuron*. 2017;96(3):697–708. <https://doi.org/10.1016/j.neuron.2017.09.056>.
- Frankel DH, Hanusa BH, Zitelli JA. New primary nonmelanoma skin cancer in patients with a history of squamous cell carcinoma of the skin. Implications and recommendations for follow-up. *J Am Acad Dermatol*. 1992;26(5):720–6. [https://doi.org/10.1016/0190-9622\(92\)70100-T](https://doi.org/10.1016/0190-9622(92)70100-T).
- Davalos D, Grutzendler J, Yang G, Kim JV, Zuo Y, Jung S, et al. ATP mediates rapid microglial response to local brain injury in vivo. *Nature Neuroscience*. 2005;8(6):752–8. <https://doi.org/10.1038/nn1472>.
- Peri F, Nüsslein-Volhard C. Live imaging of neuronal degradation by microglia reveals a role for v0-ATPase a1 in phagosomal fusion in vivo. *Cell*. 2008;133(5):916–27. <https://doi.org/10.1016/j.cell.2008.04.037>.
- Sofroniew MV. Multiple roles for astrocytes as effectors of cytokines and inflammatory mediators. *The Neuroscientist: A Review Journal Bringing Neurobiology, Neurology and Psychiatry*. 2014;20(2):160–72. <https://doi.org/10.1177/1073858413504466>.
- Damisah EC, Hill RA, Rai A, Chen F, Rothlin CV, Ghosh S, et al. Astrocytes and microglia play orchestrated roles and respect phagocytic territories during neuronal corpse removal in vivo. *Sci Adv*. 2020;6:eaba3239.
- Rostami J, Holmqvist S, Lindström V, Sigvardson J, Westermark GT, Ingelsson M, et al. Human astrocytes transfer aggregated alpha-synuclein via tunneling nanotubes. *J Neurosci*. 2017;37(49):11835–53. <https://doi.org/10.1523/JNEUROSCI.0983-17.2017>.
- Söllvander S, Nikitidou E, Brolin R, Söderberg L, Sehlin D, Lannfelt L, et al. Accumulation of amyloid-β by astrocytes result in enlarged endosomes and microvesicle-induced apoptosis of neurons. *Molecular Neurodegeneration*. 2016;11(1):38. <https://doi.org/10.1186/s13024-016-0098-z>.
- Marín-Teva JL, Dusart I, Colin C, Gervais A, van Rooijen N, Mallat M. Microglia promote the death of developing Purkinje cells. *Neuron*. 2004;41(4):535–47. [https://doi.org/10.1016/S0896-6273\(04\)00069-8](https://doi.org/10.1016/S0896-6273(04)00069-8).
- Ali Khan MA, Yousef SA, Mullins CE. Percutaneous transluminal balloon pulmonary valvuloplasty for the relief of pulmonary valve stenosis with special reference to double-balloon technique. *American Heart Journal*. 1986;112(1):158–66. [https://doi.org/10.1016/0002-8703\(86\)90695-2](https://doi.org/10.1016/0002-8703(86)90695-2).
- Gadani SP, Walsh JT, Smirnov I, Zheng J, Kipnis J. The glia-derived alarmin IL-33 orchestrates the immune response and promotes recovery following CNS injury. *Neuron*. 2015;85(4):703–9. <https://doi.org/10.1016/j.neuron.2015.01.013>.
- Liddelov SA, Guttenplan KA, Clarke LE, Bennett FC, Bohlen CJ, Schirmer L, et al. Neurotoxic reactive astrocytes are induced by activated microglia. *Nature*. 2017;541(7638):481–7. <https://doi.org/10.1038/nature21029>.
- Shi Q, Chowdhury S, Ma R, Le KX, Hong S, Calderone BJ, et al. Complement C3 deficiency protects against neurodegeneration in aged plaque-rich APP/PS1 mice. *Sci Transl Med*. 2017;9(392):eaaf6295. <https://doi.org/10.1126/scitranslmed.aaf6295>.
- Rothhammer V, Borucki DM, Tjon EC, Takenaka MC, Chao C-C, Ardura-Fabregat A, et al. Microglial control of astrocytes in response to microbial metabolites. *Nature*. 2018;557(7707):724–8. <https://doi.org/10.1038/s41586-018-0119-x>.
- Batlle M, Ferri L, Andrade C, Ortega F-J, Vidal-Taboada JM, Pugliese M, et al. Astroglia-microglia cross talk during neurodegeneration in the rat hippocampus. *Biomed Res Int*. 2015;2015:102419.
- Lian H, Litvinchuk A, Chiang AC-A, Aithmitti N, Jankowsky JL, Zheng H. Astrocyte-microglia cross talk through complement activation modulates amyloid pathology in mouse models of Alzheimer's disease. *J Neurosci*. 2016;36(2):577–89. <https://doi.org/10.1523/JNEUROSCI.2117-15.2016>.
- Wu T, Dejanovic B, Gandham VD, Gogineni A, Edmonds R, Schauer S, et al. Complement C3 is activated in human AD brain and is required for neurodegeneration in mouse models of amyloidosis and tauopathy. *Cell Rep*. 2019;28:2111–2123.e6.
- Liddelov SA, Marsh SE, Stevens B. Microglia and astrocytes in disease: dynamic duo or partners in crime? *Trends in Immunology*. 2020;41(9):820–35. <https://doi.org/10.1016/j.it.2020.07.006>.
- Lindström V, Gustafsson G, Sanders LH, Howlett EH, Sigvardson J, Kasravan A, et al. Extensive uptake of α-synuclein oligomers in astrocytes results in sustained intracellular deposits and mitochondrial damage. *Mol Cell Neurosci*. 2017;82:143–56. <https://doi.org/10.1016/j.mcn.2017.04.009>.
- Rostami J, Fotaki G, Sirois J, Mzezewa R, Bergström J, Essand M, et al. Astrocytes have the capacity to act as antigen-presenting cells in the Parkinson's disease brain. *Journal of Neuroinflammation*. 2020;17(1):119. <https://doi.org/10.1186/s12974-020-01776-7>.
- Falk A, Koch P, Kesavan J, Takashima Y, Ladewig J, Alexander M, et al. Capture of neuroepithelial-like stem cells from pluripotent stem cells provides a versatile system for in vitro production of human neurons. *PLoS ONE*. 2012;7(1):e29597. <https://doi.org/10.1371/journal.pone.0029597>.
- Lundin A, Delsing L, Clausen M, Ricchiuto P, Sanchez J, Sabirsh A, et al. Human iPSC-derived astroglia from a stable neural precursor state show improved functionality compared with conventional astrocytic models. *Stem Cell Reports*. 2018;10(3):1030–45. <https://doi.org/10.1016/j.stemcr.2018.01.021>.
- McQuade A, Coburn M, Tu CH, Hasselmann J, Davtyan H, Blurton-Jones M. Development and validation of a simplified method to generate human microglia from pluripotent stem cells. *Molecular Neurodegeneration*. 2018;13(1):67. <https://doi.org/10.1186/s13024-018-0297-x>.
- Beretta C, Nikitidou E, Streubel-Gallasch L, Ingelsson M, Sehlin D, Erlandsson A. Extracellular vesicles from amyloid-β exposed cell cultures induce severe dysfunction in cortical neurons. *Sci Rep*. 2020;10(1):19656. <https://doi.org/10.1038/s41598-020-72355-2>.
- Nikitidou E, Khoonsari PE, Shevchenko G, Ingelsson M, Kultima K, Erlandsson A. Increased release of apolipoprotein E in extracellular vesicles following amyloid-β protofibril exposure of neuroglial co-cultures. *J Alzheimers Dis*. 2017;60(1):305–21. <https://doi.org/10.3233/JAD-170278>.
- Nixon RA, Yang D-S, Lee J-H. Neurodegenerative lysosomal disorders: a continuum from development to late age. *Autophagy*. 2008;4(5):590–9. <https://doi.org/10.4161/auto.6259>.
- Nixon RA. Autophagy, amyloidogenesis and Alzheimer disease. *Journal of Cell Science*. 2007;120(23):4081–91. <https://doi.org/10.1242/jcs.019265>.
- Appelqvist H, Wäster P, Kågedal K, Öllinger K. The lysosome: from waste bag to potential therapeutic target. *Journal of Molecular Cell Biology*. 2013;5(4):214–26. <https://doi.org/10.1093/jmcb/mjt022>.
- Verkhatsky A, Matteoli M, Parpura V, Mochly J-P, Zorec R. Astrocytes as secretory cells of the central nervous system: idiosyncrasies of vesicular secretion. *The EMBO Journal*. 2016;35(3):239–57. <https://doi.org/10.15252/embj.201592705>.
- Park J, Wetzel I, Marriotti I, Dréau D, D'Avanzo C, Kim DY, et al. A 3D human microglia system modeling neurodegeneration and neuroinflammation in Alzheimer's disease. *Nat Neurosci*. 2018;21(7):941–51. <https://doi.org/10.1038/s41593-018-0175-4>.

## Publisher's Note

Springer Nature remains neutral with regard to jurisdictional claims in published maps and institutional affiliations.